

## Data Set

The time interval between samples is approximately 3-4 seconds and each time series is approximately 100-300 seconds of post-stimulation data. Table 1 shows a summary of the knockdown data used for statistical parameter estimation for this model in addition to the wild-type experiments.

Cell Line	Measured Fraction Knockdown		Model Value						Sample Size		
	qRT-PCR	Western	Nominal	Lower	Upper	<10nM	C5a		UDP		
							10 - 100nM	>100nM	<1μM	1 - 10μM	> 10μM
Wild-type	-	-	-	-	-	4	8	3	5	5	4
GRK2 (2)	90% ± 7%, n=5	40% ± 6%, n=6	40.0%	22.0%	58.0%	2	12	2	3	1	5
Gai2 (3)	83% ± 5%, n=4	73% ± 6%, n=5	73.0%	55.0%	91.0%	-	5	-	5	-	7
Gaq (3)	70% ± 8%, n=7	66% ± 23%, n=2	66.0%	0.0%	95.0%	-	3	-	1	-	3
PLCb3 (1)	-	n=3	83.0%	38.0%	100.0%	-	3	-	-	-	3
PLCb4 (1)	87% ± 6%, n=5	-	87.0%	69.0%	100.0%	-	4	-	4	-	4

Table 1: The data set used for parameter estimation is shown in this table. Five different cell lines which have a perturbation in the level of a key signal transduction protein were constructed by shRNAi lentiviral infection. The calcium response from these cell lines in addition to the wild-type cell line were used to fit relevant parameters in the model. Since shRNAi does not entirely remove the protein product, the fraction knockdown was estimated by qRT-PCR and by Western blot analysis. The standard error (se) was computed for each estimate and the upper and lower confidence intervals were computed as  $\pm 3 \cdot se$ . The knockdown confidence intervals are used in the GPCR model to construct prediction confidence intervals for the calcium response. Where several cell lines were constructed for each knockdown, the best was selected and reported in parenthesis. The sample size for each knockdown-ligand dose combination is shown in the last 6 columns.

This data set was first used to check the accuracy of the model. The five knockdown perturbations and the range of ligand doses impose strong quantitative constraints on the model.

## Model & Data Preprocessing

From the vantage point of an average cell, the concentration of ligand is at first zero, then as the ligand molecules diffuse in the media the effective concentration at the membrane interface asymptotes to the equilibrium concentration. We employ the following model for the ligand concentration at the plasma membrane interface as a function of time

$$y(t) = \begin{cases} \frac{a_1(t-t_0)}{(t-t_0)+a_2} + a_3 & t > t_0 \\ a_3 & t \leq t_0 \end{cases}$$

and fit parameters of the model using FITC measurements as described in the supplementary information. Figure S5 shows the fit of the model to the FITC data.

Fura-2 measurements report only the relative change in cytosolic calcium and are not able to report absolute calcium levels. In order that the baseline concentration of cytosolic calcium in our model match a reasonable resting cytosolic calcium concentration we subtracted the average the prestimulus calcium concentration for each experiment and recentered the baseline at 80nM which is a reasonable physiological level for these cells.

In our model we have lumped PLC $\beta$ 2 and PLC $\beta$ 3 because their regulators and effectors in the context of the rest of the calcium model are identical. However, the experimental perturbations of PLC $\beta$ 3 left PLC $\beta$ 2

concentrations unchanged. Accordingly, we took the knockdown fraction to be 50% of that reported by western blot analysis for the purposes of simulation of PLC $\beta$ 3 knockdown experiments.

## Detailed Statistical Inference

Twenty of the 84 parameters were chosen to be estimated from data based on relevance to the experimental data. Only those parameters that related to the knockdown experiments in the data set were estimated and are denoted with a star in Table S2. We used data to estimate only the two forward rate constants in the enzymatic mass-action equations because the forward and reverse rate constants for a given reaction will be highly correlated in the posterior distribution making estimation by Markov chain methods computationally expensive.

For each estimated parameter we constructed an independent Gaussian prior on a log scale with a mean chosen based on relevant literature and a standard deviation of 0.25. We found that this prior variance was sufficiently permissive to the exploration of the space while still constraining the rates to be physically reasonable. The prior distribution over the parameters allows the incorporation of both soft and hard constraints in the parameter estimates. Parameter sets with zero measure are not permitted in the posterior distribution and parameter sets with small measure must be assigned a large likelihood in order to have a large posterior probability.

The likelihood function links the prior distribution with the posterior distribution under Bayes rule

$$\Pr(\theta | y) = \frac{p(y | \theta) \Pr(\theta)}{\Pr(y)}.$$

In our model, the likelihood function is a Gaussian distribution according to the non-linear regression equation  $y = f(\theta) + \varepsilon$ ,  $\varepsilon \sim N(0, \sigma^2)$ , where  $f(\theta)$  is the deterministic model prediction. The posterior distribution is of interest because it informs us as to the most probable setting of the parameters as well as the uncertainty in the values.

The Metropolis-Hastings algorithm (1) was used to estimate the posterior density of the parameters  $\Pr(\theta | y)$ . Since the posterior density of the parameters has significant correlation structure, three independent chains were simulated from different initial parameter values. Each chain was simulated for a burn-in period of 50,000 iterations and then a sample size of 29906 was taken with a thinning factor of 10. To assess convergence of the posterior distribution estimate, we used the Gelman-Rubin potential scale reduction factor (PSRF) (2). The multivariate PSRF is 2.44 and 95% of the individual PSRFs were less than 1.5. A PSRF value of one indicates that the distribution has converged and values near one are close to converged.

Posterior prediction confidence intervals were constructed using the percentiles from the predictive distribution approximated with 2000 Monte Carlo samples from  $\Pr(y_{\text{new}} | \theta_i)$  at each of 100 simple random samples from  $\Pr(\theta | y)$  according to

$$\Pr(y_{\text{new}} | y) = \int \Pr(y_{\text{new}} | \theta) \Pr(\theta | y) d\theta \approx \sum_{i=1}^{100} \Pr(y_{\text{new}} | \theta_i) \Pr(\theta_i | y),$$

where  $\Pr(y_{\text{new}} | \theta_i) \sim N(f(\theta), \hat{s}^2)$  and  $\hat{s}^2$  is the pooled variance estimate, which is computed as an average of the variances of all the time points in each of the 29 wild-type experiments. These average variances are weighted by the number of technical replicates in each experiment and then averaged to yield the estimate  $\hat{s}^2$ .

The observed standard deviation for each calcium measurement was obtained from 3-4 replicates on the same plate. By chance the replicate measurements for some time points were nearly identical causing the standard deviation estimate to be close to zero. Since the log of the likelihood for a Gaussian distribution contains the standard deviation estimate in the denominator, a near-zero value will force the likelihood to be very large unless a parameter value is selected which causes the simulation value to be very close to the measured value in the numerator. This effectively causes only a few terms in the likelihood to have a disproportionate importance

in the model fit. We implemented a common remedy for this situation. A small constant factor ( $1nM$ ) was added to the estimate of the standard deviation.

Figure S1:

This figure shows exemplar MCMC realizations for parameter  $k_{109f}$  (the UDP+P2YR forward binding rate) from three independent chains. The chains have converged to the stationary distribution which is the posterior distribution as measured by the PSRF (see Materials and Methods).

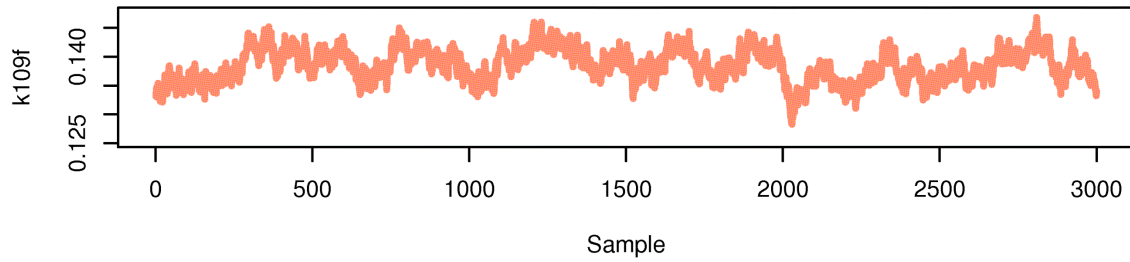
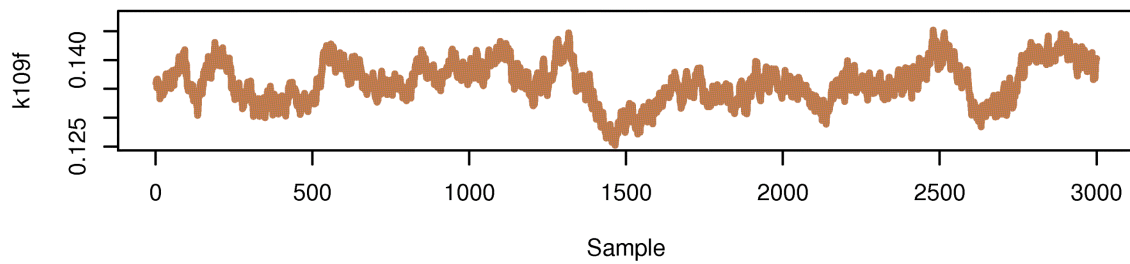
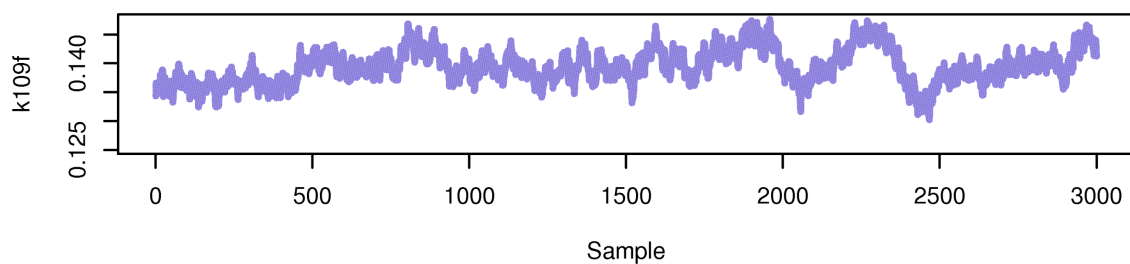


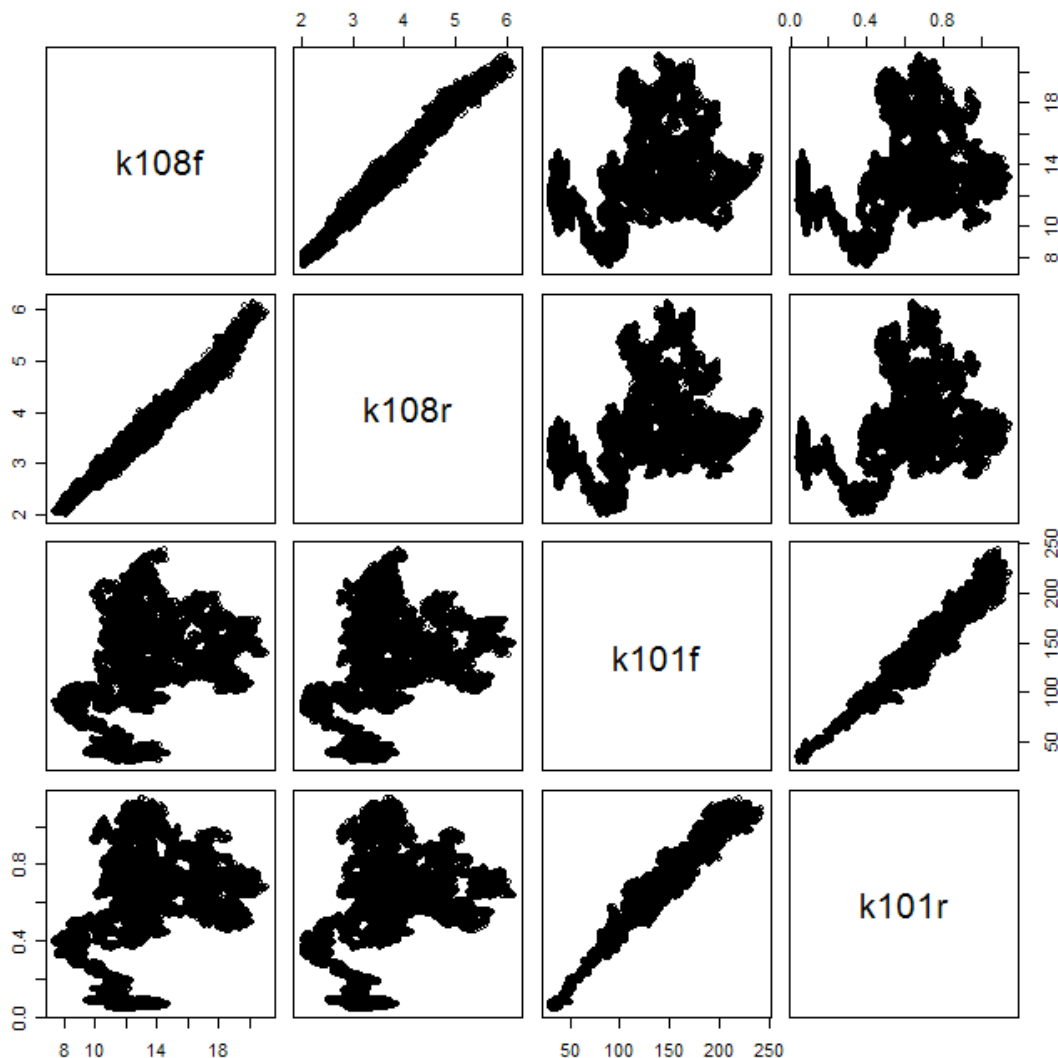
Figure S2: Posterior Distributions & Correlations

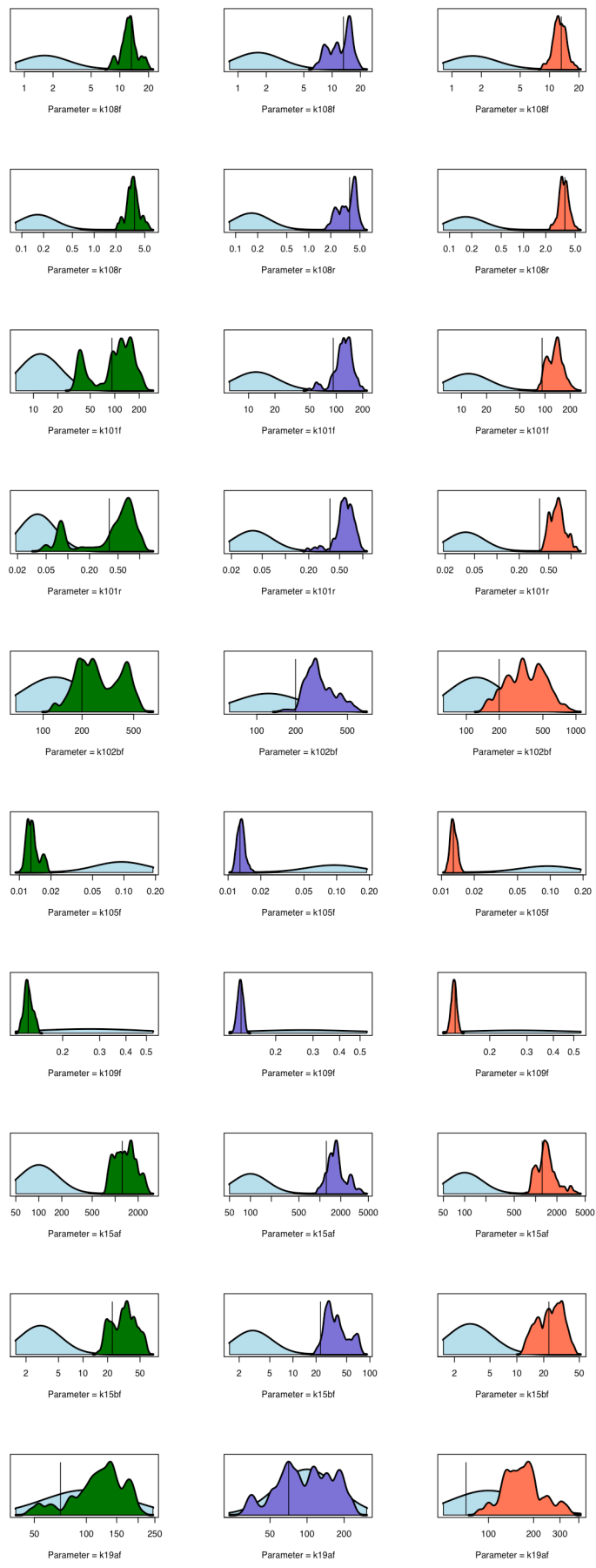
The first figure shows that the pairwise marginal posterior distributions for the ligand binding reactions for P2YR and C5aR. The posterior distributions show the dissociation constants for the reactions are tightly constrained by the data, while the values of the forward and reverse rates that make up the ratio are not as well constrained by the data.

Additionally, the UDP binding rates are not correlated with the C5a binding rates.  $k_{108f}$  and  $k_{108r}$  are the P2YR forward and reverse rates and  $k_{101f}$  and  $k_{101r}$  are the C5aR rates.

The next two figures show the one-way marginal posterior density estimates from three independent MCMC chains with approximately 30,000 samples. The 20 estimates parameters are along the rows and the independent chains are along the columns. In each plot, the light blue density is the prior density and the green, purple and orange densities are the posterior densities. The vertical line shows the parameter value used in the model simulations in the paper and listed in table S3. All of the densities are plotted on a log scale.

Each marginal posterior distribution estimate is constructed from independent MCMC chains. The results from each chain (three of them) are shown in the columns of the second figure below. In some cases the algorithm sampled heavily from one mode that was not explored as heavily by another chain. However, the PSRF criterion used to assay convergence and a visual inspection of overall posterior density correspondence do indicate that the posterior distributions are sufficiently sampled by all three chains in aggregate. Furthermore, the fit of the model to the data as shown in figure S3 shows that the model point estimates are effective in fitting the actual calcium measurements.





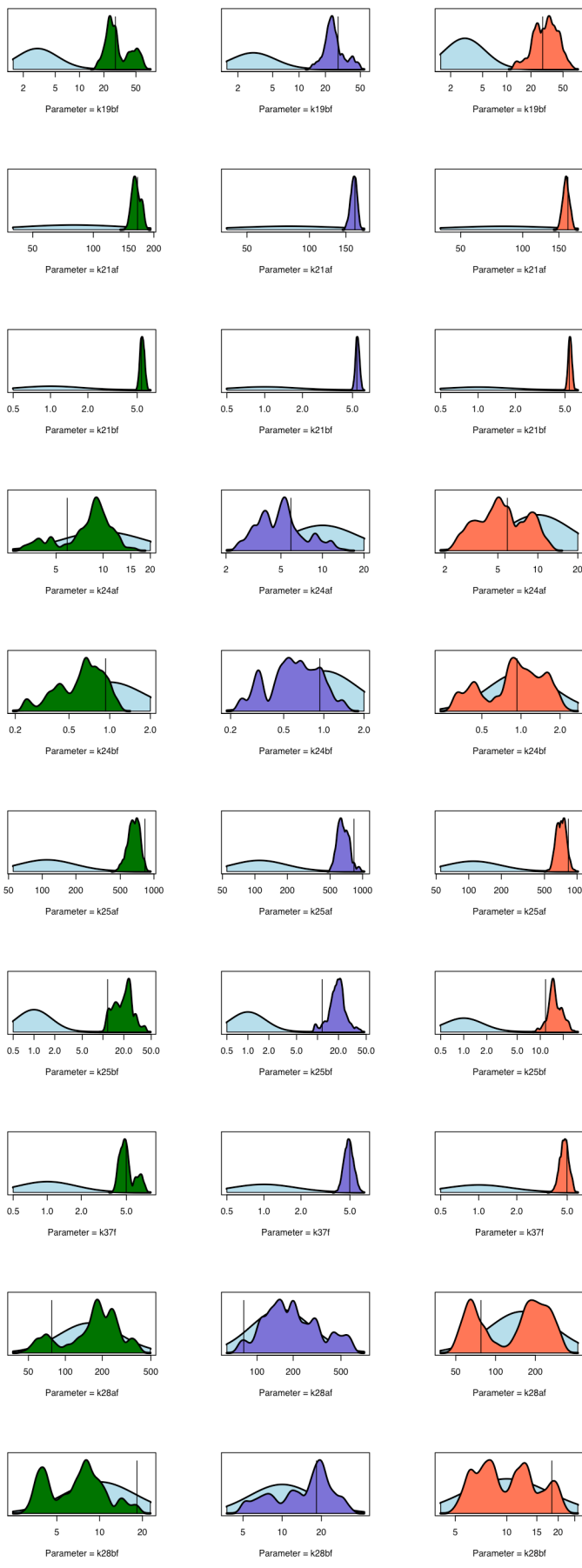
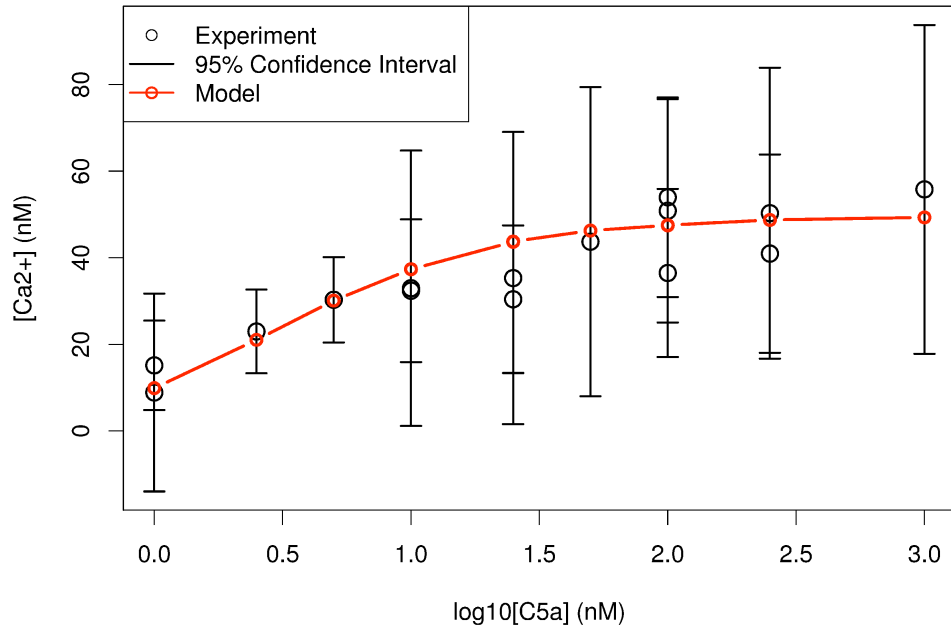


Figure S3: Peak Height Dose Response

This figure shows the single ligand calcium dose responses for C5a and UDP stimulation.

### Wild-type C5a peak height dose response



### Wild-type UDP peak height dose response

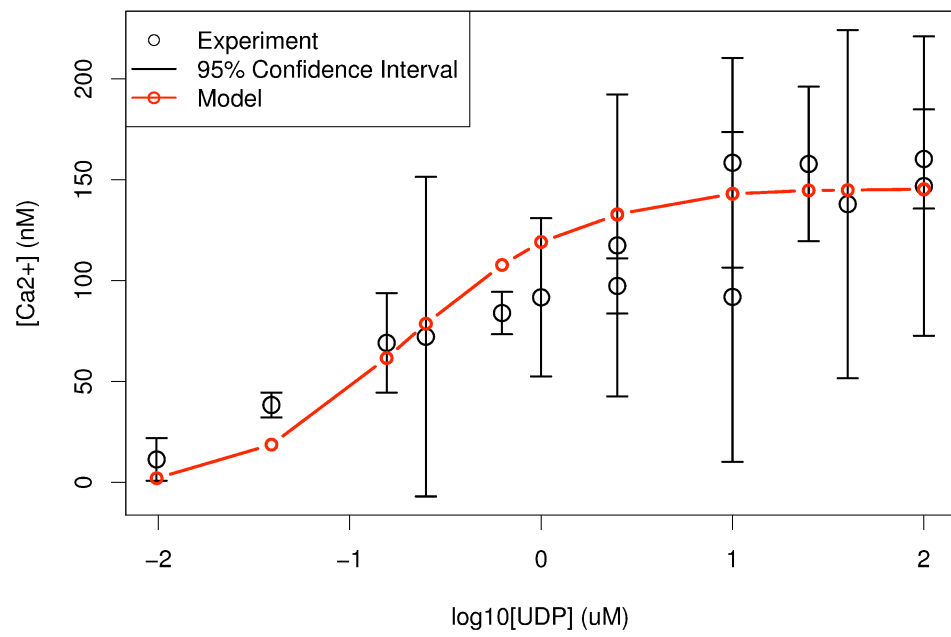
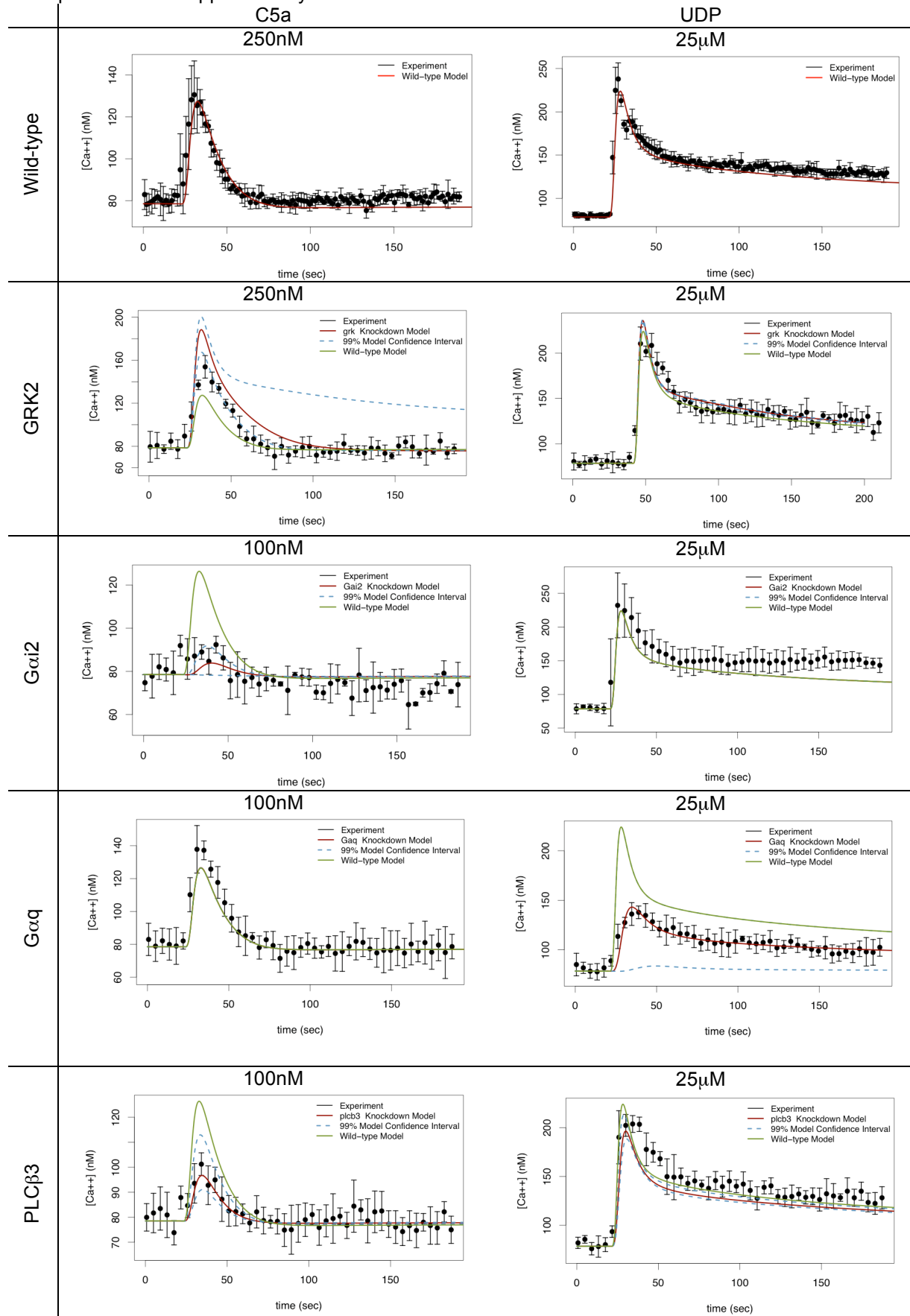


Figure S4: Knockdown Simulations

This figure shows representative simulations and data for each knockdown experiment. A complete set of all 96 experiments is provided in a supplementary folder.



**PLC $\beta$ 4**

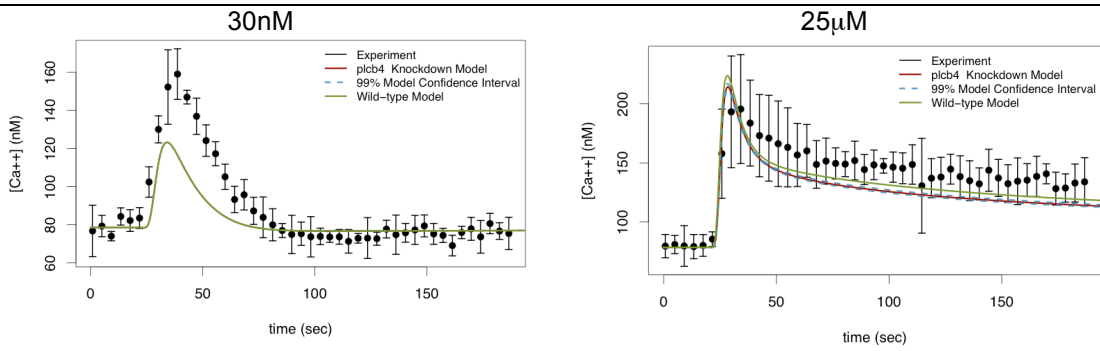


Figure S5: Input Model Fit

This figure shows the input model (described in Materials and Methods) fit to the FITC measurements. The ligand concentration that the cell sees does not transit instantaneously from 0 to the final concentration. The ligand concentration is expected to take an amount of time that is significant on the scale of the measurements made for this study to reach the final concentration.

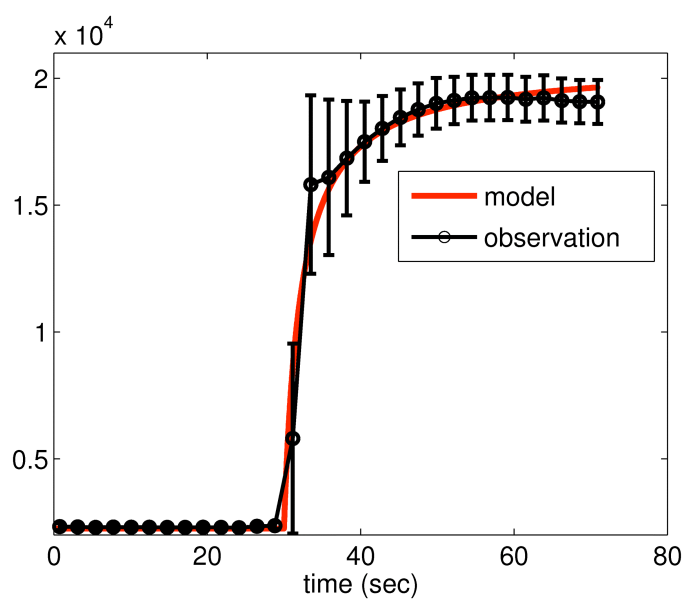


Figure S6: Large Pathway Diagram

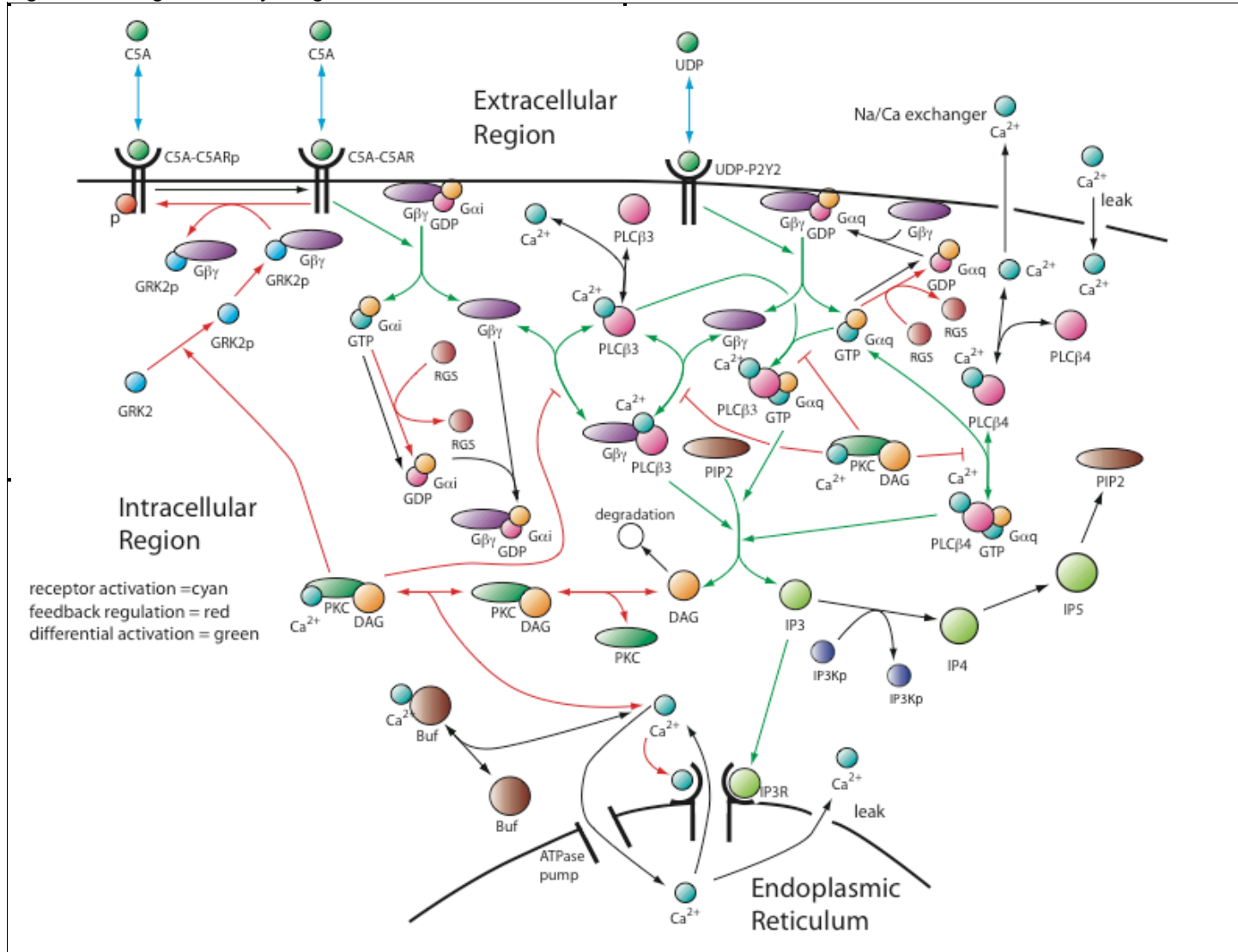
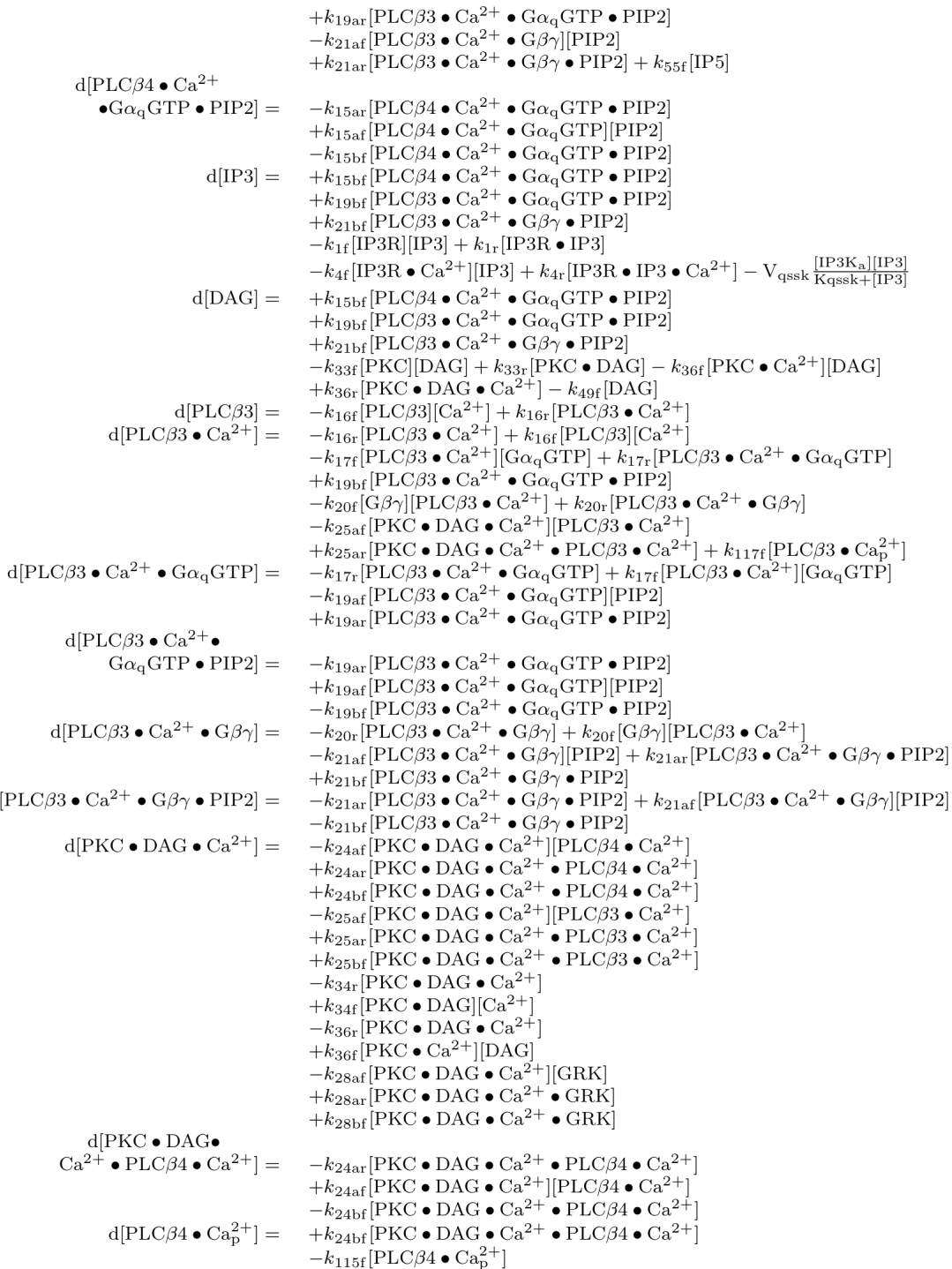


Figure S7: System of Differential Equations

This figure shows the complete set of differential equations used to simulate the model. These equations are also available in the source c code for the model supplied. This system of equations with the initial conditions and nominal parameter values reported in Tables S1 and S2 respectively completely define the model and allow for the reproduction of the simulations used in this paper on any platform.

$$\begin{aligned}
d[C5aR] &= -k_{101f}[C5a][C5aR] + k_{101r}[C5aC] + k_{104f}[C5aC_p] \\
d[C5aC] &= -k_{101r}[C5aC] + k_{101f}[C5a][C5aR] - k_{102af}[GRK_p \bullet G\beta\gamma][C5aC] \\
&\quad + k_{102ar}[GRK_p \bullet G\beta\gamma \bullet C5aC] \\
d[GRK_p \bullet G\beta\gamma] &= -k_{102af}[GRK_p \bullet G\beta\gamma][C5aC] + k_{102ar}[GRK_p \bullet G\beta\gamma \bullet C5aC] \\
&\quad + k_{102bf}[GRK_p \bullet G\beta\gamma \bullet C5aC] - k_{37r}[GRK_p \bullet G\beta\gamma] + k_{37f}[GRK_p][G\beta\gamma] \\
d[GRK_p \bullet G\beta\gamma \bullet C5aC] &= -k_{102ar}[GRK_p \bullet G\beta\gamma \bullet C5aC] + k_{102af}[GRK_p \bullet G\beta\gamma][C5aC] \\
&\quad - k_{102bf}[GRK_p \bullet G\beta\gamma \bullet C5aC] \\
d[C5aC_p] &= +k_{102bf}[GRK_p \bullet G\beta\gamma \bullet C5aC] - k_{104f}[C5aC_p] \\
d[P2YR] &= -k_{108f}[UDP][P2YR] + k_{108r}[UDPC] \\
d[UDPC] &= -k_{108r}[UDPC] + k_{108f}[UDP][P2YR] - k_{109f}[UDPC][G\beta\gamma \bullet G\alpha_q GDP] \\
&\quad + k_{109f}[UDPC][G\beta\gamma \bullet G\alpha_q GDP] \\
d[G\beta\gamma \bullet G\alpha_i GDP] &= -k_{105f}[C5aC][G\beta\gamma \bullet G\alpha_i GDP] + k_{11f}[G\alpha_i GDP][G\beta\gamma] \\
d[G\beta\gamma] &= +k_{105f}[C5aC][G\beta\gamma \bullet G\alpha_i GDP] + k_{109f}[UDPC][G\beta\gamma \bullet G\alpha_q GDP] \\
&\quad - k_{11f}[G\alpha_i GDP][G\beta\gamma] - k_{113f}[G\alpha_q GDP][G\beta\gamma] - k_{20f}[G\beta\gamma][PLC\beta3 \bullet Ca^{2+}] \\
&\quad + k_{20r}[PLC\beta3 \bullet Ca^{2+} \bullet G\beta\gamma] - k_{37f}[GRK_p][G\beta\gamma] + k_{37r}[GRK_p \bullet G\beta\gamma] \\
d[G\alpha_i GTP] &= +k_{105f}[C5aC][G\beta\gamma \bullet G\alpha_i GDP] - k_{106f}[G\alpha_i GTP] - k_{9af}[RGS_a][G\alpha_i GTP] \\
&\quad + k_{9ar}[RGS_a \bullet G\alpha_i GTP] \\
d[G\alpha_i GDP] &= +k_{106f}[G\alpha_i GTP] + k_{9bf}[RGS_a \bullet G\alpha_i GTP] - k_{11f}[G\alpha_i GDP][G\beta\gamma] \\
d[G\beta\gamma \bullet G\alpha_q GDP] &= -k_{109f}[UDPC][G\beta\gamma \bullet G\alpha_q GDP] + k_{113f}[G\alpha_q GDP][G\beta\gamma] \\
d[G\alpha_q GTP] &= +k_{109f}[UDPC][G\beta\gamma \bullet G\alpha_q GDP] - k_{110f}[G\alpha_q GTP] \\
&\quad - k_{111af}[RGS_a][G\alpha_q GTP] + k_{111ar}[RGS_a \bullet G\alpha_q GTP] \\
&\quad - k_{13f}[PLC\beta4 \bullet Ca^{2+}][G\alpha_q GTP] + k_{13r}[PLC\beta4 \bullet Ca^{2+} \bullet G\alpha_q GTP] \\
&\quad - k_{17f}[PLC\beta3 \bullet Ca^{2+}][G\alpha_q GTP] + k_{17r}[PLC\beta3 \bullet Ca^{2+} \bullet G\alpha_q GTP] \\
d[G\alpha_q GDP] &= +k_{110f}[G\alpha_q GTP] + k_{111bf}[RGS_a \bullet G\alpha_q GTP] - k_{113f}[G\alpha_q GDP][G\beta\gamma] \\
&\quad + k_{15bf}[PLC\beta4 \bullet Ca^{2+} \bullet G\alpha_q GTP \bullet PIP2] \\
&\quad + k_{19bf}[PLC\beta3 \bullet Ca \bullet G\alpha_q GTP \bullet PIP2] \\
d[RGS_a] &= -k_{9af}[RGS_a][G\alpha_i GTP] + k_{9ar}[RGS_a \bullet G\alpha_i GTP] + k_{9bf}[RGS_a \bullet G\alpha_i GTP] \\
&\quad - k_{111af}[RGS_a][G\alpha_q GTP] + k_{111ar}[RGS_a \bullet G\alpha_q GTP] \\
&\quad + k_{111bf}[RGS_a \bullet G\alpha_q GTP] \\
d[RGS_a \bullet G\alpha_i GTP] &= -k_{9ar}[RGS_a \bullet G\alpha_i GTP] + k_{9af}[RGS_a][G\alpha_i GTP] \\
&\quad - k_{9bf}[RGS_a \bullet G\alpha_i GTP] \\
d[RGS_a \bullet G\alpha_q GTP] &= -k_{111ar}[RGS_a \bullet G\alpha_q GTP] + k_{111af}[RGS_a][G\alpha_q GTP] \\
&\quad - k_{111bf}[RGS_a \bullet G\alpha_q GTP] \\
d[PLC\beta4] &= -k_{12f}[PLC\beta4][Ca^{2+}] + k_{12r}[PLC\beta4 \bullet Ca^{2+}] \\
d[Ca^{2+}] &= -k_{12f}[PLC\beta4][Ca^{2+}] + k_{12r}[PLC\beta4 \bullet Ca^{2+}] - k_{16f}[PLC\beta3][Ca^{2+}] \\
&\quad + k_{16r}[PLC\beta3 \bullet Ca^{2+}] - k_{2f}[IP3R \bullet IP3][Ca^{2+}] + k_{2r}[IP3R \bullet IP3 \bullet Ca^{2+}] \\
&\quad - k_{3f}[IP3R][Ca^{2+}] + k_{3r}[IP3R \bullet Ca^{2+}] - k_{6f}[Ca^{2+}][Buf] \\
&\quad + k_{6r}[Ca^{2+} \bullet Buf] - k_{34f}[PKC \bullet DAG][Ca^{2+}] + k_{34r}[PKC \bullet DAG \bullet Ca^{2+}] \\
&\quad - k_{35f}[PKC][Ca^{2+}] + k_{35r}[PKC \bullet Ca^{2+}] \\
&\quad + c_2(v_1[IP3R \bullet IP3]^4 + v_8)([Ca_{ER}^{2+}] - [Ca^{2+}])v_4 \frac{[Ca^{2+}]^2}{[Ca^{2+}]^2 + k_4^2} \\
&\quad + a_1 - V_{ex} \frac{[Ca^{2+}]}{K_{ex} + [Ca^{2+}]} \\
d[PLC\beta4 \bullet Ca^{2+}] &= -k_{12r}[PLC\beta4 \bullet Ca^{2+}] + k_{12f}[PLC\beta4][Ca^{2+}] \\
&\quad - k_{13f}[PLC\beta4 \bullet Ca^{2+}][G\alpha_q GTP] \\
&\quad + k_{13r}[PLC\beta4 \bullet Ca^{2+} \bullet G\alpha_q GTP] \\
&\quad + k_{15bf}[PLC\beta4 \bullet Ca^{2+} \bullet G\alpha_q GTP \bullet PIP2] \\
&\quad - k_{24af}[PKC \bullet DAG \bullet Ca^{2+}][PLC\beta4 \bullet Ca^{2+}] \\
&\quad + k_{24ar}[PKC \bullet DAG \bullet Ca^{2+} \bullet PLC\beta4 \bullet Ca^{2+}] + k_{115f}[PLC\beta4 \bullet Ca_p^{2+}] \\
d[PLC\beta4 \bullet Ca^{2+} \bullet G\alpha_q GTP] &= -k_{13r}[PLC\beta4 \bullet Ca^{2+} \bullet G\alpha_q GTP] + k_{13f}[PLC\beta4 \bullet Ca^{2+}][G\alpha_q GTP] \\
&\quad - k_{15af}[PLC\beta4 \bullet Ca^{2+} \bullet G\alpha_q GTP][PIP2] \\
&\quad + k_{15ar}[PLC\beta4 \bullet Ca^{2+} \bullet G\alpha_q GTP \bullet PIP2] \\
d[PIP2] &= -k_{15af}[PLC\beta4 \bullet Ca^{2+} \bullet G\alpha_q GTP][PIP2] \\
&\quad + k_{15ar}[PLC\beta4 \bullet Ca^{2+} \bullet G\alpha_q GTP \bullet PIP2] \\
&\quad - k_{19af}[PLC\beta3 \bullet Ca^{2+} \bullet G\alpha_q GTP][PIP2]
\end{aligned}$$



$d[PKC \bullet DAG]$	$-k_{25ar}[PKC \bullet DAG \bullet Ca^{2+} \bullet PLC\beta_3 \bullet Ca^{2+}]$
$Ca^{2+} \bullet PLC\beta_3 \bullet Ca^{2+}$	$+k_{25af}[PKC \bullet DAG \bullet Ca^{2+}][PLC\beta_3 \bullet Ca^{2+}]$ $-k_{25bf}[PKC \bullet DAG \bullet Ca^{2+} \bullet PLC\beta_3 \bullet Ca^{2+}]$ $+k_{25bf}[PKC \bullet DAG \bullet Ca^{2+} \bullet PLC\beta_3 \bullet Ca^{2+}]$
$d[PLC\beta_3 \bullet Ca_p^{2+}]$	$-k_{117f}[PLC\beta_3 \bullet Ca^{2+} \bullet p]$
$d[IP3R]$	$-k_{1f}[IP3R][IP3]$ $+k_{1r}[IP3R \bullet IP3] - k_{3f}[IP3R][Ca^{2+}]$ $+k_{3r}[IP3R \bullet Ca^{2+}]$
$d[IP3R \bullet IP3]$	$-k_{1r}[IP3R \bullet IP3]$ $+k_{1f}[IP3R][IP3] - k_{2f}[IP3R \bullet IP3][Ca^{2+}]$ $+k_{2r}[IP3R \bullet IP3 \bullet Ca^{2+}]$ $-k_{2r}[IP3R \bullet IP3 \bullet Ca^{2+}]$
$d[IP3R \bullet IP3 \bullet Ca^{2+}]$	$+k_{2f}[IP3R \bullet IP3][Ca^{2+}] - k_{4r}[IP3R \bullet IP3 \bullet Ca^{2+}]$ $+k_{4f}[IP3R \bullet Ca^{2+}][IP3]$
$d[IP3R \bullet Ca^{2+}]$	$-k_{3r}[IP3R \bullet Ca^{2+}]$ $+k_{3r}[IP3R][Ca^{2+}] - k_{4f}[IP3R \bullet Ca^{2+}][IP3]$ $+k_{4r}[IP3R \bullet IP3 \bullet Ca^{2+}]$
$d[Buf]$	$-k_{6f}[Ca^{2+}][Buf] + k_{6r}[Ca^{2+} \bullet Buf]$
$d[Ca^{2+} \bullet Buf]$	$-k_{6r}[Ca^{2+} \bullet Buf] + k_{6f}[Ca^{2+}][Buf]$
$d[Ca_{ER}^{2+}]$	$-(v_1[IP3R \bullet IP3]^4 + v8)([Ca_{ER}^{2+}] - [Ca^{2+}])$ $+(1/c_2)v_4 \frac{[Ca^{2+}]^2}{[Ca^{2+}]^2 + k_4^2}$
$d[PKC]$	$-k_{33f}[PKC][DAG] + k_{33r}[PKC \bullet DAG]$ $-k_{35f}[PKC][Ca^{2+}] + k_{35r}[PKC \bullet Ca^{2+}]$
$d[PKC \bullet DAG]$	$-k_{33r}[PKC \bullet DAG]$ $+k_{33f}[PKC][DAG] - k_{34f}[PKC \bullet DAG][Ca^{2+}]$ $+k_{34r}[PKC \bullet DAG \bullet Ca^{2+}]$
$d[PKC \bullet Ca^{2+}]$	$-k_{35r}[PKC \bullet Ca^{2+}]$ $+k_{35f}[PKC][Ca^{2+}] - k_{36f}[PKC \bullet Ca^{2+}][DAG]$ $+k_{36r}[PKC \bullet DAG \bullet Ca^{2+}]$
$d[GRKp]$	$-k_{37f}[GRKp][G\beta\gamma] + k_{37r}[GRKp \bullet G\beta\gamma]$ $+k_{28bf}[PKC \bullet DAG \bullet Ca^{2+} \bullet GRK]$
$d[GRK]$	$-k_{28af}[PKC \bullet DAG \bullet Ca^{2+}][GRK] + k_{28ar}[PKC \bullet DAG \bullet Ca^{2+} \bullet GRK]$
$d[PKC \bullet DAG \bullet Ca^{2+} \bullet GRK]$	$-k_{28ar}[PKC \bullet DAG \bullet Ca^{2+} \bullet GRK] + k_{28af}[PKC \bullet DAG \bullet Ca^{2+}][GRK]$ $-k_{28bf}[PKC \bullet DAG \bullet Ca^{2+} \bullet GRK]$
$d[DAG_d]$	$+k_{49f}[DAG]$
$d[IP3K_a]$	0
$d[IP4]$	$+Vqssk50 \frac{[IP3K_a][IP3]}{K_{qssk50} + [IP3]} - V_{maxk54} \frac{[IP4]}{K_{mk54} + [IP4]}$
$d[IP5]$	$+V_{maxk54} \frac{[IP4]}{K_{mk54} + [IP4]} - k_{55f}[IP5]$

Figure S8: Hill function self-synergy. Consider a Hill function,  $H(x) = \frac{x^n}{x^n + K^n}$ .  $y^* = \frac{x^*}{K}$  is a dimensionless critical concentration  $y^*$ , below which self-synergy will occur. Based on the analysis, we conclude that: (i)  $n$  must be greater than 1 for self-synergy to occur, (ii) self synergy never occurs if the concentration  $x$  exceeds equilibrium constant  $K$  ( $y > 1$ ), and (iii) for  $n > 2$ , there is a large range of concentration for self-synergy. In the G protein model,  $x$ , is the concentration of IP3-IP3R,  $H(x)$  is the rate of change in cytosolic calcium concentration and  $n=4$ .

We have tested the validity of this self synergy hypothesis by stimulating the cells with both 20nM UDP and 40nM UDP (data not shown). Though at such low ligand concentrations, the measurement variability is high, we observed that the synergy ratio, on average was 1.17 compared to a value of 1.25 predicted by the model.

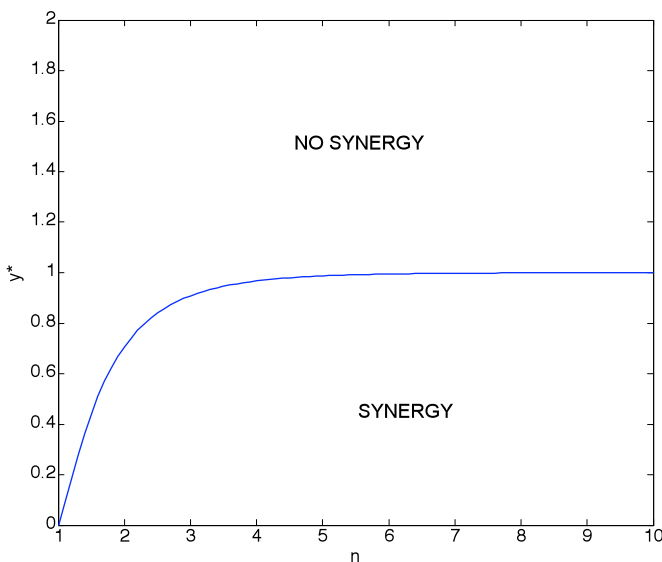


Figure S9: Parameter Sensitivity Analysis. The parameter of interest is varied by 10% while all other parameters are kept constant. The parameters are grouped according to their functionalities. The sensitivity coefficient is the ratio of the relative change in the peak height to the relative change in the parameter value. The four most sensitive parameters (sensitivity coefficient > 2) in the  $\text{Ca}_{\text{cyt}}$  category are Vqssk50 (IP3+IP3K\_a  $\rightarrow$  IP4+IP3K\_a (Vmax)), Kqssk50 (IP3+IP3K\_a  $\rightarrow$  IP4+IP3K\_a (Km)), a1 (Ca leak into the cell from outside), and Kex (Na/Ca exchange activation const). The top 3 most sensitive parameters in the PLC $\beta$ 3 category are: k21bf\* (PLC $\beta$ 3\_Ca\_Gbg\_PIP2  $\rightarrow$  PLC $\beta$ 3\_Ca\_Gbg+IP3+DAG), k20f (Gbg+PLC $\beta$ 3\_Ca  $\rightarrow$  PLC $\beta$ 3\_Ca\_Gbg), k21af\* (PLC $\beta$ 3\_Ca\_Gbg+PIP2  $\rightarrow$  PLC $\beta$ 3\_Ca\_Gbg\_PIP2). A star next to the parameter name indicates it was estimated.

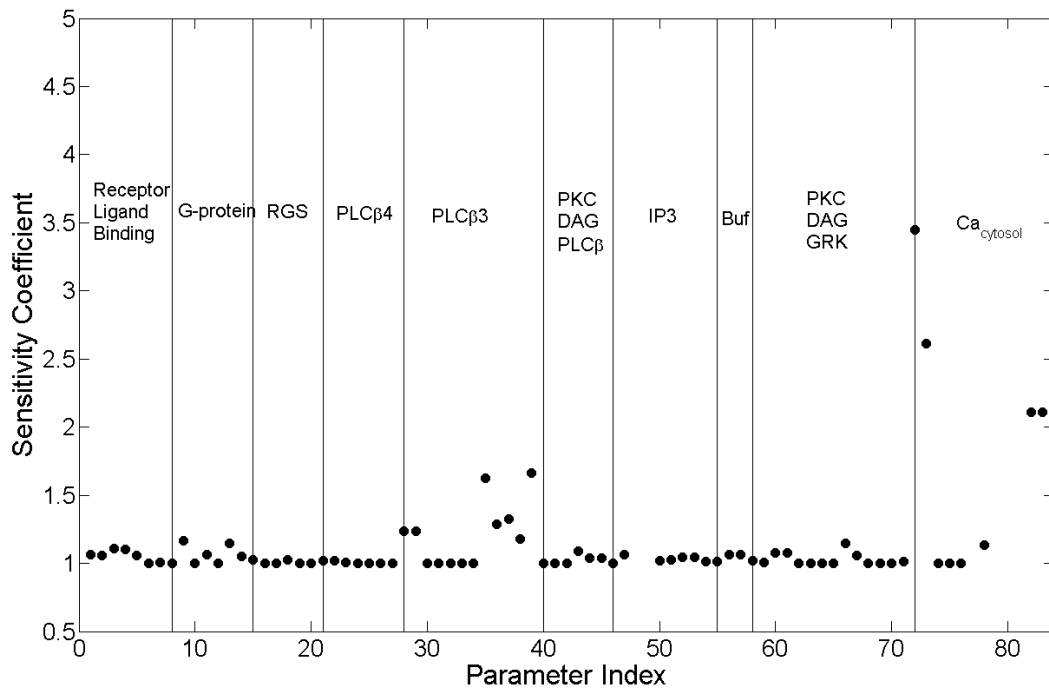


Table S1: Model Initial Conditions

This table shows the initial conditions used for the model. The model was run for sufficient time for the species states in the model to reach equilibrium before ligand stimulation was added. The number of molecules was calculated using a cell volume of 1pL.

<b>Name</b>	<b>Initial Value (<math>\mu\text{M}</math>)</b>	<b>Molecules</b>	<b>Description</b>
c5aR	5.00E-02	30100	C5a receptor concentration
p2yr	1.00E-01	60200	P2Y receptor concentration
G $\beta$ $\gamma$	7.14E+00	4299990	G $\beta$ $\gamma$ concentration
G $\alpha$ i_GDP	6.64E+00	3999989	G $\alpha$ i concentration
G $\alpha$ q_GDP	4.98E-01	300001	G $\alpha$ q concentration
PLC $\beta$ 3	1.16E-01	70001	PLC $\beta$ 3 concentration
PLC $\beta$ 4	6.64E-02	40000	PLC $\beta$ 4 concentration
PIP2	5.00E-01	301000	
IP3	1.80E-03	1084	Free IP3 concentration
DAG	1.00E-03	602	Free DAG concentration
IP3R	2.08E-02	12492	IP3 receptor concentration
IP3R-IP3	1.75E-03	1054	
IP3R-IP3-Ca	2.30E-03	1385	
IP3R-Ca	2.00E-04	120	
Ca	7.86E-02	47317	Cytosolic Calcium concentration IP3 sensitive stored calcium concentration
CaER	1.04E+01	6231302	
PKC	2.49E-02	15000	
GRK	2.31E-02	13880	GRK concentration
RGS_a	2.31E-02	13880	Regulator of G protein Signaling
Buf	4.50E-01	270599	
CaBuf	5.05E-02	30401	
IP3K_a	1.66E-03	1000	
IP4	1.00E-01	60200	
IP5	1.00E-01	60200	

Table S2: Model Parameters

This table shows the nominal parameters used for the model. Parameter distributions that were estimated are shown as shaded rows and with a star next to the parameter name in the table. The prior distribution for each parameter is as described in the Materials and Methods section with mean value specified by the column labeled "prior".

Constant	Prior	Nominal	Unit	Description
k108f*	1.628	13.20	$\mu\text{M}^{-1}\text{s}^{-1}$	UDP+p2yr -> UDPC
k108r*	0.165	3.61	s-1	UDP+p2yr <- UDPC
k101f*	12.143	92.41	$\mu\text{M}^{-1}\text{s}^{-1}$	c5a+c5aR -> c5aC
k101r*	0.0378	0.376	s-1	c5a+c5aR <- c5aC
k102af	591.54	591.54	$\mu\text{M}^{-1}\text{s}^{-1}$	GRKp_Gbg+c5aC -> GRKp_Gbg_c5aC
k102ar	12.367	12.36	s-1	GRKp_Gbg+c5aC <- GRKp_Gbg_c5aC
k102bf*	123.31	199.31	s-1	GRKp_Gbg_c5aC -> GRKp_Gbg+c5aCp
k104f	0.0001	0.0001	s-1	c5aCp -> c5aR+c5a
k105f*	0.0945	0.012	$\mu\text{M}^{-1}\text{s}^{-1}$	c5aC+Gbg_Gai_GDP -> c5aC+Gbg+Gai_GTP
k106f	0.0222	0.0222	s-1	Gai_GTP -> Gai_GDP
				UDPC+Gbg_Gaq_GDP ->
k109f*	0.2686	0.137	$\mu\text{M}^{-1}\text{s}^{-1}$	UDPC+Gbg+Gaq_GTP
k110f	0.0222	0.0222	s-1	Gaq_GTP -> Gaq_GDP
k11f	7000	7000	$\mu\text{M}^{-1}\text{s}^{-1}$	Gai_GDP+Gbg -> Gbg_Gai_GDP
k113f	7000	7000	$\mu\text{M}^{-1}\text{s}^{-1}$	Gaq_GDP+Gbg -> Gbg_Gaq_GDP
k9af	100	100	$\mu\text{M}^{-1}\text{s}^{-1}$	RGS_a+Gai_GTP -> RGS_a_Gai_GTP
k9ar	0.1	0.1	s-1	RGS_a+Gai_GTP <- RGS_a_Gai_GTP
k9bf	100	100	s-1	RGS_a_Gai_GTP -> RGS_a+Gai_GDP
k111af	100	100	$\mu\text{M}^{-1}\text{s}^{-1}$	RGS_a+Gaq_GTP -> RGS_a_Gaq_GTP
k111ar	0.1	0.1	s-1	RGS_a+Gaq_GTP <- RGS_a_Gaq_GTP
k111bf	100	100	s-1	RGS_a_Gaq_GTP -> RGS_a+Gaq_GDP
k12f	20	20	$\mu\text{M}^{-1}\text{s}^{-1}$	PLCb4+Ca -> PLCb4_Ca
k12r	8	8	s-1	PLCb4+Ca <- PLCb4_Ca
k13f	62.55	62.55	$\mu\text{M}^{-1}\text{s}^{-1}$	PLCb4_Ca+Gaq_GTP -> PLCb4_Ca_Gaq_GTP
k13r	10.632	10.63	s-1	PLCb4_Ca+Gaq_GTP <- PLCb4_Ca_Gaq_GTP
				PLCb4_Ca_Gaq_GTP+PIP2 ->
k15af*	100	1238.78	$\mu\text{M}^{-1}\text{s}^{-1}$	PLCb4_Ca_Gaq_GTP_PIP2
				PLCb4_Ca_Gaq_GTP+PIP2 <-
k15ar	1	1	s-1	PLCb4_Ca_Gaq_GTP_PIP2
				PLCb4_Ca_Gaq_GTP_PIP2 ->
k15bf*	3	22.85	s-1	PLCb4_Ca+Gaq_GDP+IP3+DAG
k16f	20	20	$\mu\text{M}^{-1}\text{s}^{-1}$	PLCb3+Ca -> PLCb3_Ca
k16r	8	8	s-1	PLCb3+Ca <- PLCb3_Ca
k17f	50	50	$\mu\text{M}^{-1}\text{s}^{-1}$	PLCb3_Ca+Gaq_GTP -> PLCb3_Ca_Gaq_GTP
k17r	0.1	0.1	s-1	PLCb3_Ca+Gaq_GTP <- PLCb3_Ca_Gaq_GTP
				PLCb3_Ca_Gaq_GTP+PIP2 ->
k19af*	100	70.87	$\mu\text{M}^{-1}\text{s}^{-1}$	PLCb3_Ca_Gaq_GTP_PIP2
				PLCb3_Ca_Gaq_GTP+PIP2 <-
k19ar	1	1	s-1	PLCb3_Ca_Gaq_GTP_PIP2
				PLCb3_Ca_Gaq_GTP_PIP2 ->
k19bf*	3	27.89	s-1	PLCb3_Ca+Gaq_GDP+IP3+DAG
k20f	8.346	8.346	$\mu\text{M}^{-1}\text{s}^{-1}$	Gbg+PLCb3_Ca -> PLCb3_Ca_Gbg
k20r	0.388	0.388	s-1	Gbg+PLCb3_Ca <- PLCb3_Ca_Gbg
				PLCb3_Ca_Gbg+PIP2 ->
k21af*	80	165.83	$\mu\text{M}^{-1}\text{s}^{-1}$	PLCb3_Ca_Gbg_PIP2
				PLCb3_Ca_Gbg+PIP2 <-
k21ar	8	8	s-1	PLCb3_Ca_Gbg_PIP2
				PLCb3_Ca_Gbg_PIP2 ->
k21bf*	1	5.41	s-1	PLCb3_Ca_Gbg+IP3+DAG
				PKC_DAG_Ca+PLCb4_Ca ->
k24af	10	5.89	$\mu\text{M}^{-1}\text{s}^{-1}$	PKC_DAG_Ca_PLCb4_Ca
				PKC_DAG_Ca+PLCb4_Ca <-
k24ar	11	11	s-1	PKC_DAG_Ca_PLCb4_Ca

Constant	Prior	Nominal	Unit	Description
k24bf	1	0.93	s-1	PKC_DAG_Ca_PLCb4_Ca -> PKC_DAG_Ca+PLCb4_Ca_p PKC_DAG_Ca+PLCb3_Ca ->
k25af	110	830.44	μM-1 s-1	PKC_DAG_Ca_PLCb3_Ca PKC_DAG_Ca+PLCb3_Ca -<- PKC_DAG_Ca_PLCb3_Ca
k25ar	11	11	s-1	PKC_DAG_Ca_PLCb3_Ca PKC_DAG_Ca+PLCb3_Ca ->
k25bf	1	11.69	s-1	PKC_DAG_Ca+PLCb3_Ca_p
k115f	0.12	0.12	s-1	PLCb4_Ca_p -> PLCb4_Ca
k117f	0.12	0.12	s-1	PLCb3_Ca_p -> PLCb3_Ca
k1f	177.47	177.47	μM-1 s-1	IP3R+IP3 -> IP3R_IP3
k1r	2.2	2.2	s-1	IP3R+IP3 -<- IP3R_IP3
k2f	0.411	0.411	μM-1 s-1	IP3R_IP3+Ca -> IP3R_IP3_Ca
k2r	0.0434	0.0434	s-1	IP3R_IP3+Ca -<- IP3R_IP3_Ca
k3f	0.9	0.9	μM-1 s-1	IP3R+Ca -> IP3R_Ca
k3r	0.806	0.806	s-1	IP3R+Ca -<- IP3R_Ca
k4f	20	20	μM-1 s-1	IP3R_Ca+IP3 -> IP3R_IP3_Ca
k4r	0.029	0.029	s-1	IP3R_Ca+IP3 -<- IP3R_IP3_Ca (thermcycle)
k6f	10	10	μM-1 s-1	Ca+Buf -> CaBuf
k6r	7	7	s-1	Ca+Buf -<- CaBuf
k33f	100	100	μM-1 s-1	PKC+DAG -> PKC_DAG
k33r	0.05	0.05	s-1	PKC+DAG -<- PKC_DAG
k34f	10	10	μM-1 s-1	PKC_DAG+Ca -> PKC_DAG_Ca
k34r	6	6	s-1	PKC_DAG+Ca -<- PKC_DAG_Ca (thermcycle)
k35f	0.01	0.01	μM-1 s-1	PKC+Ca -> PKC_Ca
k35r	30	30	s-1	PKC+Ca -<- PKC_Ca
k36f	1000	1000	μM-1 s-1	PKC_Ca+DAG -> PKC_DAG_Ca
k36r	0.0001	0.0001	s-1	PKC_Ca+DAG -<- PKC_DAG_Ca
k37f	1	4.98	μM-1 s-1	GRKp+Gbg -> GRKp_Gbg
k37r	0.05	0.05	s-1	GRKp+Gbg -<- GRKp_Gbg
k28af	158.49	77.52	μM-1 s-1	PKC_DAG_Ca+GRK -> PKC_DAG_Ca_GRK
k28ar	10	10	s-1	PKC_DAG_Ca+GRK -<- PKC_DAG_Ca_GRK
k28bf	10	18.34	s-1	PKC_DAG_Ca_GRK -> PKC_DAG_Ca+GRKp
k49f	0.35	0.35	s-1	DAG -> DAG_d
Vqssk50	13.9	13.9	s-1	IP3+IP3K_a -> IP4+IP3K_a (Vmax)
Kqssk50	0.055	0.055	μM	IP3+IP3K_a -> IP4+IP3K_a (Km)
Vmaxk54	100	100	μM s-1	IP4 -> IP5
Kmk54	1.4	1.4	μM	IP4 -> IP5
k55f	0.008	0.008	s-1	IP5 -> PIP2
c2	0.185	0.185	none	ratio of ER volume/cell: de young
v1	1E8	1E8	s-1	Ca channel flux constant
v8	0.15	0.15	s-1	leak flux constant
v4	20	20	μM s-1	maximum Ca uptake rate (SERCA)
k4	0.65	0.65	μM	activation constant of SERCA pump
a1	0.0055	0.0055	μM s-1	Ca leak into the cell from outside
Kex	0.25	0.25	μM	Na/Ca exchange activation const
Vex	0.023	0.023	μM s-1	maximum Ca exchange rate

Table S3: Parameter Posterior Uncertainty and References

This table shows the HPD intervals as computed by the R CODA library function "hpdiinterval". HPD intervals for each of the three MCMC chains were calculated and the union of those intervals is reported for each parameter in this table. The prior value reported in Table S2 was set using information from references listed in the appropriate column. The references used to form the basis of the parameter estimates are shown in the last column. A detailed discussion of the choice of rate constant estimates is shown in (3).

		Parameter HPD Interval				
		mean	lower 95%	upper 95%	model	Reference
k108f*	UDP+p2yr -> UDPC	12.85	6.64	18.47	13.20	
k108r*	UDP+p2yr <- UDPC	3.54	1.88	5.01	3.62	
k101f*	c5a+c5aR -> c5aC	134.61	32.34	197.77	92.41	
k101r*	c5a+c5aR <- c5aC	0.67	0.04	1.00	0.38	
k102af	GRKp_Gbg+c5aC -> GRKp_Gbg_c5aC	591.54	591.54	591.54	591.54	
k102ar	GRKp_Gbg+c5aC <- GRKp_Gbg_c5aC	12.37	12.37	12.37	12.37	
k102bf*	GRKp_Gbg_c5aC <- GRKp_Gbg+c5aCp	378.66	118.54	660.84	199.31	
k104f	c5aCp -> c5aR+c5a	1.00E-04	1.00E-04	1.00E-04	1.00E-04	
	c5aC+Gbg_Gai_GDP ->					
k105f*	c5aC+Gbg_Gai_GTP	1.30E-02	1.09E-02	1.79E-02	1.29E-02	
k106f	Gai_GTP -> Gai_GDP	0.02	0.02	0.02	0.02	
	UDPC+Gbg_Gaq_GDP ->					
k109f*	UDPC+Gbg_Gaq_GTP	1.36E-01	1.26E-01	1.51E-01	1.37E-01	
k110f	Gaq_GTP -> Gaq_GDP	0.02	0.02	0.02	0.02	
k11f	Gai_GDP+Gbg -> Gbg_Gai_GDP	7000.00	7000.00	7000.00	7000.00	
k113f	Gaq_GDP+Gbg -> Gbg_Gaq_GDP	7000.00	7000.00	7000.00	7000.00	
k9af	RGS_a+Gai_GTP -> RGS_a_Gai_GTP	100.00	100.00	100.00	100.00	
k9ar	RGS_a+Gai_GTP <- RGS_a_Gai_GTP	0.10	0.10	0.10	0.10	
k9bf	RGS_a_Gai_GTP -> RGS_a+Gai_GDP	100.00	100.00	100.00	100.00	
k111af	RGS_a+Gaq_GTP -> RGS_a_Gaq_GTP	100.00	100.00	100.00	100.00	
k111ar	RGS_a+Gaq_GTP <- RGS_a_Gaq_GTP	0.10	0.10	0.10	0.10	
k111bf	RGS_a_Gaq_GTP -> RGS_a+Gaq_GDP	100.00	100.00	100.00	100.00	
k12f	PLCb4+Ca -> PLCb4_Ca	20.00	20.00	20.00	20.00	(4, 5)
k12r	PLCb4+Ca <- PLCb4_Ca	8.00	8.00	8.00	8.00	(4, 5)
k13f	PLCb4_Ca+Gaq_GTP ->	62.55	62.55	62.55	62.55	(6, 7)
k13r	PLCb4_Ca+Gaq_GTP <-	10.63	10.63	10.63	10.63	(6, 7)
	PLCb4_Ca_Gaq_GTP+PIP2 ->					
k15af*	PLCb4_Ca+Gao_GTP_PIP2	1497.23	764.53	3041.57	1238.79	(6, 7)
	PLCb4_Ca_Gaq_GTP+PIP2 <-					
k15ar	PLCb4_Ca+Gao_GTP_PIP2	1.00	1.00	1.00	1.00	(6, 7)
k15bf*	PLCb4_Ca+Gao_GTP_PIP2 ->	24.77	12.11	69.52	22.85	(6, 7)
k16f	PLCb3+Ca -> PLCb3_Ca	20.00	20.00	20.00	20.00	(4, 5, 8, 9)
k16r	PLCb3+Ca <- PLCb3_Ca	8.00	8.00	8.00	8.00	(4, 5, 8, 9)
k17f	PLCb3_Ca_Gaq_GTP ->	50.00	50.00	50.00	50.00	(10, 11)
k17r	PLCb3_Ca_Gaq_GTP <-	0.10	0.10	0.10	0.10	(10, 11)
	PLCb3_Ca_Gaq_GTP+PIP2 ->					
k19af*	PLCb3_Ca_Gao_GTP_PIP2	176.85	30.58	302.61	70.88	(10)
	PLCb3_Ca_Gao_GTP_PIP2 <-					
k19ar	PLCb3_Ca_Gao_GTP_PIP2	1.00	1.00	1.00	1.00	(10)
k19bf*	PLCb3_Ca_Gao_GTP_PIP2 ->	32.19	12.24	56.67	27.90	(10)
k20f	Gbg+PLCb3_Ca -> PLCb3_Ca_Gbg	8.35	8.35	8.35	8.35	(10, 12-15)
k20r	Gbg+PLCb3_Ca <- PLCb3_Ca_Gbg	0.39	0.39	0.39	0.39	(10, 12-15)
k21af*	PLCb3_Ca_Gbg_PIP2 ->	162.54	149.74	179.55	165.83	(10, 12-15)
	PLCb3_Ca_Gbg_PIP2 <-					
k21ar	PLCb3_Ca_Gbg_PIP2	8.00	8.00	8.00	8.00	(10, 12-15)
	PLCb3_Ca_Gbg_PIP2 ->					
k21bf*	PLCb3_Ca_Gbg+IP3+DAG	5.49	5.09	5.90	5.42	(10, 12-15)
	PKC_DAG_Ca+PLCb4_Ca ->					
k24af*	PKC_DAG_Ca_PLCb4_Ca	5.92	2.31	12.55	5.90	
	PKC_DAG_Ca+PLCb4_Ca <-					
k24ar	PKC_DAG_Ca_PLCb4_Ca	11.00	11.00	11.00	11.00	
	PKC_DAG_Ca+PLCb4_Ca_p ->					
k24bf*	PKC_DAG_Ca+PLCb4_Ca_p	1.00	0.22	1.84	0.93	
	PKC_DAG_Ca+PLCb3_Ca ->					
k25af*	PKC_DAG_Ca+PLCb3_Ca	716.37	513.98	856.07	830.44	

	PKC_DAG_Ca_PLCb3_Ca					
k25ar	PKC_DAG_Ca+PLCb3_Ca <-	11.00	11.00	11.00	11.00	
	PKC_DAG_Ca_PLCb3_Ca					
	PKC_DAG_Ca_PLCb3_Ca ->					
k25bf*	PKC_DAG_Ca+PLCb3_Ca_p	15.95	9.04	32.19	11.70	
k115f	PLCb4_Ca_p -> PLCb4_Ca	0.12	0.12	0.12	0.12	
k117f	PLCb3_Ca_p -> PLCb3_Ca	0.12	0.12	0.12	0.12	
k1f	IP3R+IP3 -> IP3R_IP3	177.47	177.47	177.47	177.47	(16, 17)
k1r	IP3R+IP3 <- IP3R_IP3	2.20	2.20	2.20	2.20	(16, 17)
k2f	IP3R_IP3+Ca -> IP3R_IP3_Ca	0.41	0.41	0.41	0.41	(16, 17)
k2r	IP3R_IP3+Ca <- IP3R_IP3_Ca	0.04	0.04	0.04	0.04	(16, 17)
k3f	IP3R+Ca -> IP3R_Ca	0.90	0.90	0.90	0.90	(16, 17)
k3r	IP3R+Ca <- IP3R_Ca	0.81	0.81	0.81	0.81	(16, 17)
k4f	IP3R_Ca+IP3 -> IP3R_IP3_Ca	20.00	20.00	20.00	20.00	(16, 17)
k4r	IP3R_Ca+IP3 <- IP3R_IP3_Ca (thermcycle)	0.03	0.03	0.03	0.03	(16, 17)
k6f	Ca+Buf -> CaBuf	10.00	10.00	10.00	10.00	
k6r	Ca+Buf <- CaBuf	7.00	7.00	7.00	7.00	
k33f	PKC+DAG -> PKC_DAG	100.00	100.00	100.00	100.00	(18, 19)
k33r	PKC+DAG <- PKC_DAG	0.05	0.05	0.05	0.05	(18, 19)
k34f	PKC_DAG+Ca -> PKC_DAG_Ca	10.00	10.00	10.00	10.00	(18, 19)
	PKC_DAG+Ca <- PKC_DAG_Ca					
k34r	(thermcycle)	6.00	6.00	6.00	6.00	(18, 19)
k35f	PKC+Ca -> PKC_Ca	0.01	0.01	0.01	0.01	(18, 19)
k35r	PKC+Ca <- PKC_Ca	30.00	30.00	30.00	30.00	(18, 19)
k36f	PKC_Ca+DAG -> PKC_DAG_Ca	1000.00	1000.00	1000.00	1000.00	(18, 19)
k36r	PKC_Ca+DAG <- PKC_DAG_Ca	0.00	0.00	0.00	1.00E-04	(18, 19)
k37f*	GRKp+Gbg -> GRKp_Gbg	4.76	3.97	6.94	4.98	(20, 21)
k37r	GRKp+Gbg <- GRKp_Gbg	0.05	0.05	0.05	0.05	(20, 21)
k28af*	PKC_DAG_Ca+GRK -> PKC_DAG_Ca_GRK	155.61	47.79	529.50	77.52	(22)
k28ar	PKC_DAG_Ca+GRK <- PKC_DAG_Ca_GRK	10.00	10.00	10.00	10.00	(22)
	PKC_DAG_Ca_GRK ->					
k28bf*	PKC_DAG_Ca+GRKp	10.85	2.96	28.80	18.35	(22)
k49f	DAG -> DAG_d	0.35	0.35	0.35	0.35	
Vqssk50	IP3+IP3K_a -> IP4+IP3K_a (Vmax)	13.9	13.90	13.90	13.9	(23)
Kqssk50	IP3+IP3K_a -> IP4+IP3K_a (Km)	0.0557	0.06	0.06	0.0557	(23)
Vmaxk54	IP4 -> IP5	100	100.00	100.00	100	(4)
Kmk54	IP4 -> IP5	1.4	1.40	1.40	1.4	
k55f	IP5 -> PIP2	0.008	0.01	0.01	0.008	
c2	ratio of ER volume/cell: de young	0.185	0.19	0.19	0.185	(16, 17)
v1	Ca channel flux constant	1.00E+08	1.00E+08	1.00E+08	1.00E+08	(16, 17)
v8	leak flux constant	0.15	0.15	0.15	0.15	
v4	maximum Ca uptake rate (SERCA)	20	20.00	20.00	20	
k4	activation constant of SERCA pump	0.65	0.65	0.65	0.65	
a1	Ca leak into the cell from outside	0.0055	0.01	0.01	0.0055	
Kex	Na/Ca exchange activation const	0.25	0.25	0.25	0.25	
Vex	maximum Ca exchange rate	0.023	0.02	0.02	0.023	

Table S4: Goodness of Fit Evaluation

We use the mean squared error criterion to evaluate the goodness of our model fit to the data. We have used this data in the estimation procedure and thus does not constitute a true validation. However, we show that in general our model fits the bulk of the data. Those areas of lack-of-fit are usually due to extraordinary experiment-to-experiment variation and in some cases point to unaccounted mechanisms. We elaborate on one such mechanism (multiple GRK isoforms) in the text of the article.

<b>Cell Line</b>	<b>C5a Dose</b>	<b>UDP Dose</b>	<b>Sample Size</b>	<b>Avg. MSE</b>	<b>Comments</b>
Wild-type	<10nM		4	3.39E-05	Generally good fit within data errors
	10-100nM		8	2.19E-05	Slight peak overshoot
	>100nM		3	3.37E-05	Generally good fit within data errors
GRK2 Knockdown	<10nM		2	2.39E-04	Peak overshoot and slower decay than observed.
	10-100nM		12	2.75E-04	Peak overshoot by ~33%
	>100nM		2	2.33E-04	Peak overshoot by ~20%
Gai2 Knockdown	10-100nM		5	4.83E-05	4/5 within observed error
Gaq Knockdown	10-100nM		3	5.68E-05	Generally good fit
PLCb3 Knockdown	10-100nM		3	1.96E-05	Generally good fit
PLCb4 Knockdown	10-100nM		4	2.79E-04	Peak undershoot by ~25%
Wild-type		<1uM	5	7.07E-05	undershoot peak for very low [UDP] ~10-40nM
		1-10uM	5	1.32E-04	Generally fits average. Experiment to experiment variation is high.
		>10uM	4	8.05E-05	Generally good fit
GRK2 Knockdown		<1uM	3	1.56E-04	Higher than observed sustained phase. Large experimental variation.
		1-10uM	1	5.62E-04	No observed peak in data.
		>10uM	5	1.41E-03	Generally fits average. Experiment to experiment variation is high.
Gai2 Knockdown		<1uM	5	9.28E-04	Undershoots peak by ~33%.
		>10uM	7	1.31E-03	Undershoots peak by ~40%
Gaq Knockdown		<1uM	1	3.68E-05	Generally good fit within experimental error.
		>10uM	3	2.14E-04	Generally good fit.
PLCb3 Knockdown		>10uM	3	6.12E-04	Sustained phase is lower than observed.
PLCb4 Knockdown		<1uM	4	7.92E-05	Sustained phase is higher than observed.
		>10uM	4	8.79E-04	Sustained phase is lower than observed.

Protocol 1: FITC Protocol

1. FITC soln at 400nM used for robotic addition to wells. A 4-fold in-well dilution yielded 100nM final in a final 100ul well volume.
2. Wells contained 75 ul water.
3. Instrument settings:
  - Flex mode = serial reads at FITC wavelengths (495ex/ 525em, 510 cutoff)
  - Robotic additions at 20 seconds
  - Additions defined by time / volume / ejection height / ejection speed plus
  - trituration # cycles / volume / height (speed is defined by above)
4. Settings for first vs second data set were:
  - 25ul volume / 75ul height / speed 1
  - 25ul volume / 50ul height / speed 4 plus 1 trituration @ 25ul volume, 50ul height

## References

1. Robert, C. P. & Casella, G. (2004) *Monte Carlo statistical methods* (Springer, New York).
2. Gelman, A. & Rubin, D. B. (1992) *Statistical Science* **7**, 457-472.
3. Flaherty, P. J. (2006) PhD Thesis in Electrical Engineering and Computer Sciences, University of California, Berkeley; *A Kinetic Model for G protein-coupled Signal Transduction in Macrophage Cells*, UCB/EECS-2007-4, <http://www.eecs.berkeley.edu/Pubs/TechRpts/2007/EECS-2007-4.html>.
4. Berg, J. M., Tymoczko, J. L., Stryer, L. & National Center for Biotechnology Information (U.S.) (2002) (W.H. Freeman; NCBI, Bethesda, MD).
5. Ellis, M. V., James, S. R., Perisic, O., Downes, C. P., Williams, R. L. & Katan, M. (1998) *J Biol Chem* **273**, 11650-9.
6. Lee, C. W., Lee, K. H., Lee, S. B., Park, D. & Rhee, S. G. (1994) *J Biol Chem* **269**, 25335-8.
7. Jiang, H., Wu, D. & Simon, M. I. (1994) *J Biol Chem* **269**, 7593-6.
8. Ryu, S. H., Cho, K. S., Lee, K. Y., Suh, P. G. & Rhee, S. G. (1987) *J Biol Chem* **262**, 12511-8.
9. Meyer, T. & Stryer, L. (1988) *Proc Natl Acad Sci U S A* **85**, 5051-5.
10. Jiang, H., Kuang, Y., Wu, Y., Smrcka, A., Simon, M. I. & Wu, D. (1996) *J Biol Chem* **271**, 13430-4.
11. Rhee, S. G. (2001) *Annu Rev Biochem* **70**, 281-312.
12. Wu, D., Katz, A. & Simon, M. I. (1993) *Proc Natl Acad Sci U S A* **90**, 5297-301.
13. Wu, D. Q., Lee, C. H., Rhee, S. G. & Simon, M. I. (1992) *J Biol Chem* **267**, 1811-7.
14. Murthy, K. S., Coy, D. H. & Makhlof, G. M. (1996) *J Biol Chem* **271**, 23458-63.
15. Katz, A., Wu, D. & Simon, M. I. (1992) *Nature* **360**, 686-9.
16. De Young, G. W. & Keizer, J. (1992) *Proceedings of the National Academy of Sciences of the United States of America* **89**, 9895-9899.
17. Keizer, J. & De Young, G. W. (1992) *Biophys J* **61**, 649-60.
18. Ananthanarayanan, B., Stahelin, R. V., Digman, M. A. & Cho, W. (2003) *J Biol Chem* **278**, 46886-94.
19. Shinomura, T., Asaoka, Y., Oka, M., Yoshida, K. & Nishizuka, Y. (1991) *Proc Natl Acad Sci U S A* **88**, 5149-53.
20. Penela, P., Ribas, C. & Mayor, F., Jr. (2003) *Cell Signal* **15**, 973-81.
21. Daaka, Y., Pitcher, J. A., Richardson, M., Stoffel, R. H., Robishaw, J. D. & Lefkowitz, R. J. (1997) *Proc Natl Acad Sci U S A* **94**, 2180-5.
22. Chuang, T. T., LeVine, H., 3rd & De Blasi, A. (1995) *J Biol Chem* **270**, 18660-5.
23. Xia, H. J. & Yang, G. (2005) *Cell Res* **15**, 83-91.